ISPRS Journal of Photogrammetry and Remote Sensing 102 (2015) 85–95

Contents lists available at ScienceDirect

ISPRS Journal of Photogrammetry and Remote Sensing

journal homepage: www.elsevier.com/locate/isprsjprs

Evaluating leaf chlorophyll content prediction from multispectral remote sensing data within a physically-based modelling framework

H. Croft [a,*], J.M. Chen [a], Y. Zhang [b], A. Simic [c], T.L. Noland [d], N. Nesbitt [a], J. Arabian [a]

[a] University of Toronto, Department of Geography, Toronto, ON M5S 3G3, Canada
[b] Delta State University, Division of Biological and Physical Sciences, Cleveland, MS 38733, USA
[c] Bowling Green State University, Department of Geology, Bowling Green, OH 43403-0211, USA
[d] Ontario Ministry of Natural Resources, Ontario Forest Research Institute, 1235 Queen St. E., Sault Ste. Marie, ON P6A 2E5 Canada

ARTICLE INFO

Article history:
Received 6 October 2014
Received in revised form 5 December 2014
Accepted 15 January 2015
Available online 9 February 2015

Keywords:
Leaf area index
Landsat
PROSPECT
4-Scale
Spatial statistics
Radiative transfer model

ABSTRACT

Accurate modelling of leaf chlorophyll content over a range of spatial and temporal scales is central to monitoring vegetation stress and physiological condition, and vegetation response to different ecological, climatic and anthropogenic drivers. A process-based modelling approach can account for variation in other factors affecting canopy reflectance, providing a more accurate estimate of chlorophyll content across different vegetation species, time-frames, and broader spatial extents. However, physically-based modelling studies usually use hyperspectral data, neglecting a wealth of data from broadband and multispectral sources. In this study, we assessed the potential for using canopy (4-Scale) and leaf radiative transfer (PROSPECT4/5) models to estimate leaf chlorophyll content using canopy Landsat satellite data and simulated Landsat bands from leaf level hyperspectral reflectance data. Over 600 leaf samples were used to test the performance of PROSPECT for different vegetation species, including black spruce (*Picea mariana*), sugar maple (*Acer saccharum*), trembling aspen (*Populus tremuloides*) and jack pine (*Pinus banksiana*). At the leaf level, hyperspectral and simulated Landsat bands showed very similar results to laboratory measured chlorophyll ($R^2 = 0.77$ and $R^2 = 0.75$, respectively). Comparisons between PROSPECT4 modelled chlorophyll from simulated Landsat and hyperspectral spectra showed a very close correspondence ($R^2 = 0.97$, root mean square error (RMSE) = 3.01 μg/cm^2), as did simulated reflectance bands from other broadband and narrowband sensors (MODIS: $R^2 = 0.99$, RMSE = 1.80 μg/cm^2; MERIS: $R^2 = 0.97$, RMSE = 2.50 μg/cm^2 and SPOT5 HRG: $R^2 = 0.96$, RMSE = 5.38 μg/cm^2). Modelled leaf chlorophyll content from Landsat 5 TM canopy reflectance data, acquired from over 40 ground validation sites, demonstrated a strong relationship with measured leaf chlorophyll content ($R^2 = 0.78$, RMSE = 8.73 μg/cm^2, $p < 0.001$), and a high linearity with negligible systematic bias. Study results demonstrate the small number of input bands required for PROSPECT inversion and provide a theoretical and operational basis for the future retrieval of leaf chlorophyll content using broadband or multispectral sensors within a physically-based approach.

1. Introduction

Leaf chlorophyll content is a key ecological variable, both directly through its role in photosynthesis and in the conversion of solar radiation into stored chemical energy (Gitelson et al., 2006), and indirectly as a bio-indicator of plant physiological condition; highlighting areas of plant disturbance and environmental pressure (Sampson et al., 2003; Zarco-Tejada et al., 2002). The potential of leaves to absorb photosynthetically active radiation (PAR) is largely a function of foliar concentrations of photosynthetic pigments, which can affect CO_2 assimilation and primary production (Richardson et al., 2002). As a result, leaf chlorophyll content is an inherent element of water, energy and carbon cycles and is an increasingly key component within regional and global carbon models (Inoue et al., 2008). Monitoring the response of plant chlorophyll content to changing environmental and climatic conditions is also paramount for understanding and modelling ecosystem responses. However, most approaches for retrieving leaf chlorophyll content have focused on using hyperspectral or occasionally narrow-band reflectance data (Croft et al., 2014b; Zhang et al., 2008a). Little work has been devoted to multispectral or broadband

* Corresponding author.
E-mail address: holly.croft@utoronto.ca (H. Croft).

http://dx.doi.org/10.1016/j.isprsjprs.2015.01.008
0924-2716/

sensors, thereby potentially neglecting a wealth of data across a range of spatial scales and time-frames. The Landsat satellite series in particular, provides the longest running continuous collection of fine-spatial resolution imagery—dating back to Landsat 1 in 1972 and continuing with the recent launch of Landsat 8 in February 2013. This very long data time series offers the possibility of monitoring changes in forest biophysical parameters over a long time frame (Croft et al., 2014a), with a spatial resolution (30 m) that supports both the requirements of fine-spatial resolution studies and global monitoring (Kovalskyy and Roy, 2013). Other multi-spectral sensors include the Systeme Pour l'Observation de la Terre (SPOT) High-Resolution Visible (HRV), MODIS and the forthcoming Sentinel-2 and -3 multi-spectral sensors (Verrelst et al., 2012).

To take full advantage of the increasing wealth of satellite data that is available, the effect of a reduced number of bands on the accuracy of chlorophyll predictions and model inversion processes must be considered. Physically-based models provide an explicit connection between biophysical variables and canopy reflectance, through the modelling of radiation transfer within the canopy or leaf, based on physical laws. The PROSPECT leaf model (Jacquemoud and Baret, 1990) is a very popular and longstanding radiative transfer model, which in its inverse mode simulates leaf biochemical and structural properties from leaf reflectance and transmittance spectra (400–2500 nm). Since 1990, several model improvements have been undertaken, including incorporating new leaf biochemical dry matter constituents and increasing the spectral resolution to 1 nm (Feret et al., 2008). The latest versions (PROSPECT4 and 5) include a more realistic leaf surface roughness parameter and updates to the specific absorption coefficients for water, dry matter, and leaf pigments. Importantly, PROSPECT5 also incorporates a physically-based separate treatment of chlorophylls and carotenoids (Feret et al., 2008). Despite the extensive use of PROSPECT and widespread validation across several vegetation species and functional types, including broadleaf (Demarez and Gastellu-Etchegorry, 2000) and coniferous trees (Croft et al., 2013b), very few studies have used broadband data within such physically-based, radiative transfer models. Notable exceptions include the work of Houborg and Boegh (2008) and Houborg et al. (2009), who used four SPOT bands (10 m spatial resolution) to model leaf chlorophyll in agricultural crops using the ACRM canopy reflectance model (Kuusk, 1995) and PROSPECT (Jacquemoud and Baret, 1990), giving a root-mean-square deviation of 7.1 $\mu g/cm^2$. In an early study, Jacquemoud et al. (1995) tested the application of SAIL and PROSPECT for modelling sugar beet biochemical properties, using near hyperspectral AVIRIS data and simulated Landsat TM bands, finding that both data sets provided extremely similar results. Despite this positive finding, little further work has occurred using physically-based models and broadband reflectance data for chlorophyll retrieval.

In this study, we assessed the potential of using broadband satellite sensors to model leaf chlorophyll content. A linked canopy geometrical optical radiative transfer model (4-Scale) and leaf radiative model (PROSPECT) were inverted and the performance of PROSPECT compared for hyperspectral leaf reflectance factors against simulated Landsat broad bands, along with bands from other multispectral sensors. The specific objectives of this research are to:

- investigate the potential for broadband and multispectral reflectance data to model leaf chlorophyll content within a physically-based approach;
- assess the accuracy of PROSPECT modelled chlorophyll content using simulated bands from multi-spectral sensors (Landsat 5 TM, MODIS, MERIS, SPOT HRG) against hyperspectral inputs;
- compare the performance of PROSPECT4 and PROSPECT5 to model chlorophyll content from hyperspectral and multispectral reflectance data.

2. Methods

2.1. Field sites

Field sampling was conducted at three locations throughout Ontario, Canada (Haliburton Forest, Sudbury and Chapleau), representing a range of vegetation species, canopy structural conditions and ecosystem communities.

2.1.1. Haliburton forest

Haliburton forest, Ontario (45° 14′ 15.5″N, 78° 32′ 18.0″ W) is located within the Great Lakes-St. Lawrence region (Rowe, 1972), with an average annual precipitation of approximately 1050 mm and mean annual temperature of 5 °C (Gradowski and Thomas, 2006). The field site is located within a mature sugar maple stand (*Acer saccharum* M.) and is underlain by shallow brunisols or juvenile podzols (pH 4.2 to 5.1) (Gradowski and Thomas, 2006). Ground-based sampling in the sugar maple (SM) stand was carried out 7 times during the 2004 growing season from June 10th to September 30th (Zhang et al., 2007).

2.1.2. Sudbury

Black spruce (BS) and trembling aspen (TA) trees were sampled at a range of sites northwest of Sudbury, Ontario (46° 49′ 13″ N to 47° 12′ 9″ N and 81° 22′ 2″ W to 81° 54′ 30″ W; Fig. 1). Six black spruce (BS) sites were sampled in the summer of 2003 and 2004 (Zhang et al., 2008a) and 11 black spruce and two trembling aspen (TA) sites were sampled during the summer of 2007 (Simic et al., 2011). The field locations were situated at an elevation of approximately 350 m above sea level, and underlain by shallow soils on Canadian Shield bedrock. Temperatures range from −40 °C to 30 °C, with a mean annual temperature of 5 °C and mean annual precipitation of approximately 800 mm (Leithead et al., 2012). The dominant vegetation is black spruce (*Picea mariana* Mill.) with deciduous forest patches containing aspen (*Populus tremuloides* Michx). Understory species include feathery bog-moss (*Sphagnum cuspidatum*), grass and dense green moss (Zhang et al., 2008a).

2.1.3. Chapleau

Ten pure jack pine (*Pinus banksiana* Lamb.) (JP) managed stands located southeast of Chapleau, Ontario (47°36′17″N to 47°33′40″N, and 83°08′23″W to 82°43′04″W) were sampled in July, 2012. Stand ages range from approximately 15 to 90 years old. The sites were underlain by well drained silt loam soils over deep gravely sand, with mean annual temperatures of 4.6 °C and annual precipitation of 871 mm (Zhu et al., 2004). Understory species include dense moss, upland willow (*Salix humilis*), blueberry (Vaccinium spp.) and grasses. At the Chapleau sites, both old (JP old), aged between 1 and 4 years, and new growth from this growing season (JP new) of jack pine needle leaves were sampled for reflectance factors and laboratory chlorophyll analysis.

2.1.4. Ground data collection

Leaves and shoots were sampled from the upper canopy, using a shotgun or mobile canopy lift, and sealed in plastic bags at a temperature of 0 °C for further analysis (Zhang et al., 2007). Leaf reflectance and transmittance were measured with an ASD spectroradiometer Fieldspec Pro FR (Analytical Spectral Devices, Inc. Boulder, USA) attached via a fibre optic cable to a Li-Cor 1800 integrating sphere (Li-Cor 1800-12S, Li-COR, Inc., Lincoln, Nebraska, USA). Reflectance and transmittance spectra were measured using methods described by (Zhang et al., 2008a, 2007). Leaf chlorophyll was extracted using spectranalysed grade N,N-dimethylformamide, and absorbance measured at 663.8 nm, 646.8 nm, and 480 nm using a Cary-1 spectrophotometer (Wellburn, 1994).

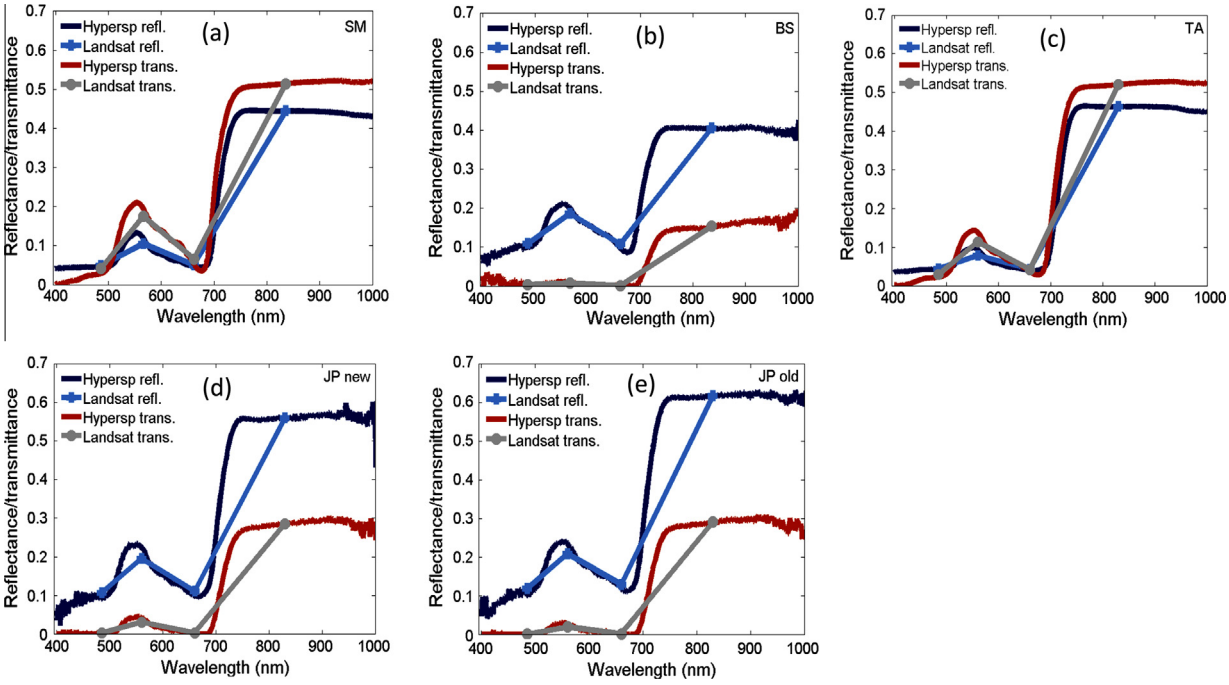

Fig. 1. Reflectance spectra for hyperspectral and Landsat bands for (a) sugar maple (SM), (b) black spruce (BS), (c) trembling aspen (TA), (d) jack pine (JP) (new), and (e) jack pine (old).

At the site level, the satellite-derived leaf chlorophyll was compared to mean ground-level chlorophyll data calculated from all leaf samples collected within each field site. Effective LAI (*Le*) was measured using the LAI-2000 plant canopy analyzer (Li-Cor, Lincoln, NE, USA) (Chen et al., 1997). The element clumping index and leaf area index were measured using TRAC (Tracing Radiation and Architecture of Canopies) (Chen and Cihlar, 1995). Structural parameters of trees (density, height and diameter breast height) were also measured and understory reflectance was measured using the ASD Fieldspec Pro Spectroradiometer for the dominant species present at each site (Croft et al., 2013b).

2.2. Landsat 5 TM data acquisition and processing

Landsat 5 TM images were radiometrically and geometrically corrected and georeferenced to UTM map projection. Landsat scenes were matched as closely as possible to the timeframe of ground data collection, within the summer growing season of each year. The Landsat scenes were atmospherically corrected using cosine estimation of atmospheric transmittance (Chavez Jr., 1996), where the cosine of sun zenith angle is used to approximate the effects of absorption by atmospheric gases and Rayleigh scattering for individual spectral bands (Eq. (1)),

$$\rho = \pi * d^2 * (L_{\lambda sat} - L_{\lambda haze})/ESUN_{\lambda} * \cos^2\theta \quad (1)$$

where p = reflectance factor; $L_{\lambda sat}$ = spectral radiance at the sensor; $L_{\lambda haze}$ = path radiance; d = earth–sun distance (AU); ESUN = mean solar exoatmospheric irradiances; θ = solar zenith angle (°). The solar exoatmospheric spectral irradiances (ESUN) for the Landsat 5 TM were obtained from Chander and Markham (2003). Path radiance ($L_{\lambda haze}$) was obtained from pixels of known zero reflectance such as large deep water bodies and it was assumed that any value in the raw image in these areas other than zero represented haze effects. This value was subsequently verified through a band specific histogram analysis by examining the step in pixel radiance values (Chavez Jr., 1988).

2.3. Modelling leaf reflectance using the 4-Scale canopy model

Foliar chlorophyll content was modelled using a canopy geometrical–optical model (Chen and Leblanc, 1997) linked with a leaf radiative transfer model (Jacquemoud and Baret, 1990). The 4-Scale model simulates the bidirectional reflectance distribution function (BRDF) based on canopy architecture at four scales: (1) tree groups, (2) tree crown geometry, (3) branches, and (4) foliage elements (Chen and Leblanc, 2001). The model considers both the structural effects of tree branches and scattering elements, the spatial distribution of tree groups, tree crowns geometries and the effects of background reflectance and shadows. Deciduous crowns are modelled as a spheroid and coniferous crowns as a cone and cylinder, both of variable dimensions. A crown is represented as a complex medium, where reflected radiance from shaded components is determined by first-order scattering (separating sunlit and shaded components), and multiple scattering from subsequent interactions with vegetation or background material (Chen and Leblanc, 2001).

The 4-Scale model was run in the forward mode, using fixed and variable structural parameters and leaf and understory reflectance spectra to model canopy reflectance. To derive leaf level reflectance, the 4-Scale model was inverted using a look-up-table (LUT) approach (Zhang et al., 2008a, 2013a,b). LUT methods are computationally efficient and can overcome the difficulty of local minima; by giving the global minimum, providing the variable space is sufficiently sampled (Jacquemoud et al., 2009). However, the 'ill-posed' problem means that different combinations of the same structural and solar/view zenith input parameters can lead to the same canopy reflectance, and consequently some *a priori* scene information is required to constrain the inversion (Kimes et al., 2000). The fixed parameters are listed in Table 1, and were based on ground measurements and reported values in the literature (e.g. Chen and Leblanc, 1997). Variable parameters included solar and viewing zenith and azimuth angles and LAI, which was derived empirically using the reduced simple ratio (RSR) following methods discussed in Croft et al. (2013b). Based on a given pixel's

Table 1
Canopy structural parameters and background component for coniferous and deciduous vegetation sites.

Parameter	Deciduous	Coniferous – Black spruce	Coniferous – Jack pine
Stem height (Ha)	10 m	5 m	5 m
Crown height (Hb)	8 m	5 m	5 m
Crown radius (R)	1.25 m	0.85 m	1.2 m
Crown shape	Spherical	Cone + cylinder	Cone + cylinder
Tree density (number per hectare)	1100	2800	3000
Neyman tree grouping factor	2	4	4
Element clumping index (ΩE)	0.95	0.89	0.89
Needle:shoot ratio (γE)	1	1.4	1.4
Element width (Ws)	0.15 m	0.04 m	0.04 m
Understory vegetation and background	Maple and wood	Soil, moss and labrador tea	Soil, moss and tealeaf willow

variable parameters, the LUT for the corresponding vegetation type was used to generate the probability of viewing the sunlit leaf (F_{PT}) and sunlit background fraction (F_{PG}) and background reflectance (ρ_{PG}) from the total scene component, and a multiple scattering factor (M) to account for multiple scattering in the tree crown (Croft et al., 2013b). From these inputs; the sunlit leaf reflectance can be modelled from the satellite or airborne derived canopy reflectance (Eq. (2)).

$$\rho_L = \frac{\rho_{\text{satellite}} - \rho_{PG} F_{PG}}{M F_{PT}} \tag{2}$$

Based on the input parameters, the 4-Scale model calculates canopy reflectance as a linear summation of four components (Chen and Leblanc, 2001): the sunlit vegetation (PT), shaded vegetation (ZT), sunlit ground (PG) and shaded ground (ZG). A multiple scattering factor is used to convert sunlit crown reflectance into sunlit leaf reflectance; accounting for the enhancement of sunlit and shaded reflectance due to multiple scattering and incorporating shaded scene components (see Zhang et al., 2008a and Croft et al., 2013b for more details).

2.4. Modelling leaf chlorophyll content using the PROSPECT model

The leaf radiative transfer model PROSPECT (Jacquemoud and Baret, 1990) was selected to generate leaf chlorophyll content using the leaf level reflectance data collected at the field sites and also from the modelled sunlit leaf reflectance derived from Landsat canopy data. Leaf optical properties (reflectance and transmittance) from 400 to 2500 nm are defined in PROSPECT4 as a function of four parameters: structure parameter, chlorophyll (a + b) concentration, dry matter content and water. PROSPECT5 also includes carotenoid content (Car) and a brown pigment parameter to represent non-photosynthetic leaf matter. Absorption is calculated as the linear summation of the specific absorption coefficients of biochemical constituents and their respective concentrations. Modelled leaf transmittance was derived from the spectral ratio of measured reflectance and transmittance for broadleaf and needle leaf samples and applied to modelled leaf reflectance (Zhang et al., 2008a). To improve PROSPECT running time and reduce the likelihood of spurious predictions using a reduced input data set, PROSPECT was inverted using bound value ranges for each of the predicted variables (Table 2). The values were set according to laboratory measurements and values reported in the literature (Feret et al., 2008).

To investigate the effects of broadband versus hyperspectral reflectance on chlorophyll retrieval by PROSPECT, Landsat TM 5 bands were simulated from hyperspectral reflectance for each sample using an ASD spectroradiometer (Section 2.1.3). The spectral response function (SRF) of a sensor describes its relative sensitivity to different wavelengths, and was used to calculate reflectance factors in simulated Landsat bands, as a weighted sum of hyperspectral reflectance and the SRF (Eq. (3)).

$$L = \sum_{\lambda=1}^{N} \beta(\lambda) L'(\lambda) \Big/ \sum_{\lambda=1}^{N} \beta(\lambda) \tag{3}$$

where L and $L'(\lambda)$ is reflectance in the larger bandwidth and reflectance data in the original wavelength and $\beta(\lambda)$ is the weight of the spectral response function (Chen et al., 2008). The PROSPECT absorption coefficients were also recalculated to the corresponding bands of the tested sensors (Table 3) using their respective spectral response functions. Whilst only visible and NIR bands are used in the inversion process, the presence of SWIR bands are also shown because of their use in the RSR index. Simulated bands have also been used to investigate the effects of different sensor bandwidths and spectral response functions on normalized difference vegetation index (NDVI) values, and to formulate corrections for biases to allow cross sensor comparisons (Steven et al., 2003).

2.5. Assessing spatial covariance between LAI and leaf chlorophyll content

To investigate the extent to which leaf chlorophyll content and LAI are spatially correlated, a bivariate local indicator of spatial autocorrelation (LISA) using Moran's I statistic was employed (Anselin, 1995). Common statistical methods such as Pearson's correlation fail to take account of spatial dependency in datasets (Anselin, 1995). Moran's I is a measure of spatial autocorrelation; defined as the likelihood that data closer together are more likely to be similar than those that are further apart (Tobler, 1965), and is a concept that underpins spatial statistical theory (Croft et al., 2013a). The local Moran's I statistic is advantageous over its global counterpart because global Moran's I only indicates the overall clustering that exists within the dataset, rather than the location of these data clusters (Anselin, 1995). Bivariate LISA gives the local correlation between a variable at a given location and the weighted average of another variable in a defined neighbourhood (Eq. (4)):

$$I_i = z_{xi} \sum_{j=1, j\neq i}^{N} w_{ij} z_{yj} \tag{4}$$

where and z_x and z_y are the standardized z-scores of variables x (LAI) and y (Chlorophyll), respectively, in district i and the neighbor-

Table 2
Bound variable ranges of modelled parameters for PROSPECT-4 and -5 inversions.

Model	N parameter	Chlorophyll (μg/cm^2)	Carotenoid (μg/cm^2)	Brown pigment	Water content (g/cm^2)	Dry matter (g/cm^2)
PROSPECT-4	1–5	0–100	–	–	0.00–0.04	0.00–0.05
PROSPECT-5	1–5	0–100	0–20	0	0.00–0.04	0.00–0.05

Table 3
The full width half maximum spectral bands of the sensors tested using simulated leaf level data in the PROSPECT model.

Sensor	Blue (nm)	Green (nm)	Red (nm)	Red-edge (nm)	NIR (nm)	SWIR (nm)
Landsat TM 5	450–520	520–600	630–690		760–900	1550–1750
MODIS	456–475	544–564	620–670		837–876	1616–1644
MERIS	407–417 437–447 485–495	505–515 555–565	615–625 660–670 677–685	703–713	750–757 773–780 855–875 880–890	
SPOT HRG		500–590	610–680		790–890	1580–1750

ing district j (Sunderlin et al., 2008). The spatial weight matrix (w_{ij}) is a binary contiguity matrix that defines the spatial structure of locations included in the calculation of the local Moran's I. A first-order contiguity matrix was used, where all observations that share a common border have $w_{ij} = 1$, otherwise $w_{ij} = 0$. LISA calculations were computed using the GeoDa software package (Anselin et al., 2006). A key feature within GeoDa is the ability to infer and map the statistical significance of spatial patterns, according to: Prob $[Li > \delta_i] \leqslant \alpha_i$, where Li is the LISA statistic at location i, δ_i is a critical value and α_i a defined significance level (Anselin, 1995), based on a randomization test. This approach compares spatially randomised reference distributions of local Moran's I values to observed values, in order to determine the probability of the observed value being obtained from a random distribution (Anselin, 1995). The threshold value of $p = 0.05$ is used to define significance.

3. Results

3.1. Hyperspectral and multispectral leaf reflectance factors for all sampled species

Representative hyperspectral reflectance factors are shown for the four vegetation species, with JP old and JP new shown separately, along with reflectance in Landsat bands simulated from the hyperspectral data using the appropriate spectral response functions. The leaf reflectance spectra exhibit considerable differences among species, with the two broadleaf species (SM and TA) displaying near-infrared (NIR) reflectance factors in the order of 0.5 although giving differences in visible wavelengths, with TA showing much lower reflectance factors and a smaller green peak. Of the needle leaf species, both old and new JP leaves gave rise to considerably higher NIR reflectance factors than those of BS.

The important differences in hyperspectral spectra in comparison to Landsat band spectra are the number of bands present, the bandwidths and the band position. The locations of the Landsat bands represent the major inflection points in the spectra (i.e., blue, green and red) although, perhaps importantly, miss the shoulder of the red edge. In terms of bandwidth effects, the greatest differences between hyperspectral and Landsat-derived reflectance occurs in green and red wavelengths, where there are larger variations in hyperspectral reflectance factor across the Landsat bandwidth (Croft et al., 2013b). The sub-band variations in reflectance are 'smoothed' by the larger Landsat bandwidth, causing simulated Landsat reflectance factors in the green band (520–600 nm) for example, to be approximately 10% lower than that in the narrowband (10 nm) reflectance at 560 nm (Croft et al., 2013b). The effect of these reduced bands and broader bandwidths on chlorophyll content modelled using PROSPECT is assessed in Section 3.3.1.

3.2. PROSPECT simulations with hyperspectral and Landsat band data

Forward runs of PROSPECT4 were performed to examine the effect of varying chlorophyll, structural parameter (N), water content (Cw) and dry matter (Cm) values on hyperspectral and Landsat reflectance spectra (Fig. 2). In the resulting modelled leaf reflectance spectra, the influence on reflectance and the wavelength dependency of the various leaf parameters are demonstrated, with the dominance of chlorophyll content in visible wavelengths and water content in the mid-infrared (>1400 nm) wavelengths. Dry matter content and leaf structure influence the entire spectrum (Ollinger, 2011).

The wavelength positions of Landsat bands coincide with the locations of the major inflection points within vegetation spectra (i.e., ≈560, 665 and the NIR); however, the top of the red-edge shoulder (≈750 nm) is missed (Landsat band centre = 835 nm). As this band has been indicated as sensitive to chlorophyll (Vogelmann et al., 1993), this departure may lead to error or uncertainty in chlorophyll prediction using Landsat bands. The coarse bandwidths in the NIR and MIR and large sampling interval leads to an absence of information from narrow features from for example, lignin or cellulose content, which affects the modelled results of structural variables (e.g., N and Cm) in particular, and also water content.

3.3. Modelled leaf-level chlorophyll content

The modelled chlorophyll values were plotted against measured leaf chlorophyll content for hyperspectral reflectance, with unfixed structural parameters (Fig. 3a and d) for JP samples, along with modelled values using fixed structural parameters (JP new – $N = 3.5$, Cm = 0.025; JP old – $N = 5$, Cm = 0.03) for hyperspectral and Landsat spectra. The structural (N) parameter is a dimensionless, integrated function of leaf thickness and leaf structure (e.g. mesophyll intercellular space) and cannot be measured empirically. Previous studies have fixed the N parameter for representative vegetation types or per individual leaf sample, based on inferences from measurements (e.g. thickness, specific leaf area) and forward simulations (Malenovský et al., 2013; Zarco-Tejada et al., 2004a). Results from PROSPECT5 present a comparable performance to PROSPECT4, both in terms of coefficient of determination (R^2) values and linearity. This is particularly surprising for the Landsat spectra, where a greater number of inversion parameters relative to a few input bands may have led to spurious predictions. The green band overlapping carotenoid and chlorophyll regions did not appear to affect the modelled chlorophyll results, although it is unlikely that Landsat bands would be able to retrieve carotenoid content due to the dominance of chlorophyll. Allowing the brown pigment parameter to vary freely resulted in considerably more scatter and several anomalous results, particularly for Landsat spectra. Once the brown pigment was set to zero, the retrievals performed well.

The results from the unfixed simulation show a large underestimation in chlorophyll content for the JP samples. The forward PROSPECT simulations (Fig. 2) illustrate the high absorbance in visible wavelengths for large chlorophyll contents, which is not consistent with the reflectance spectra (Fig. 1) resulting in the model inversion underestimating chlorophyll. However, thicker leaves (with a larger N parameter value) show increased visible

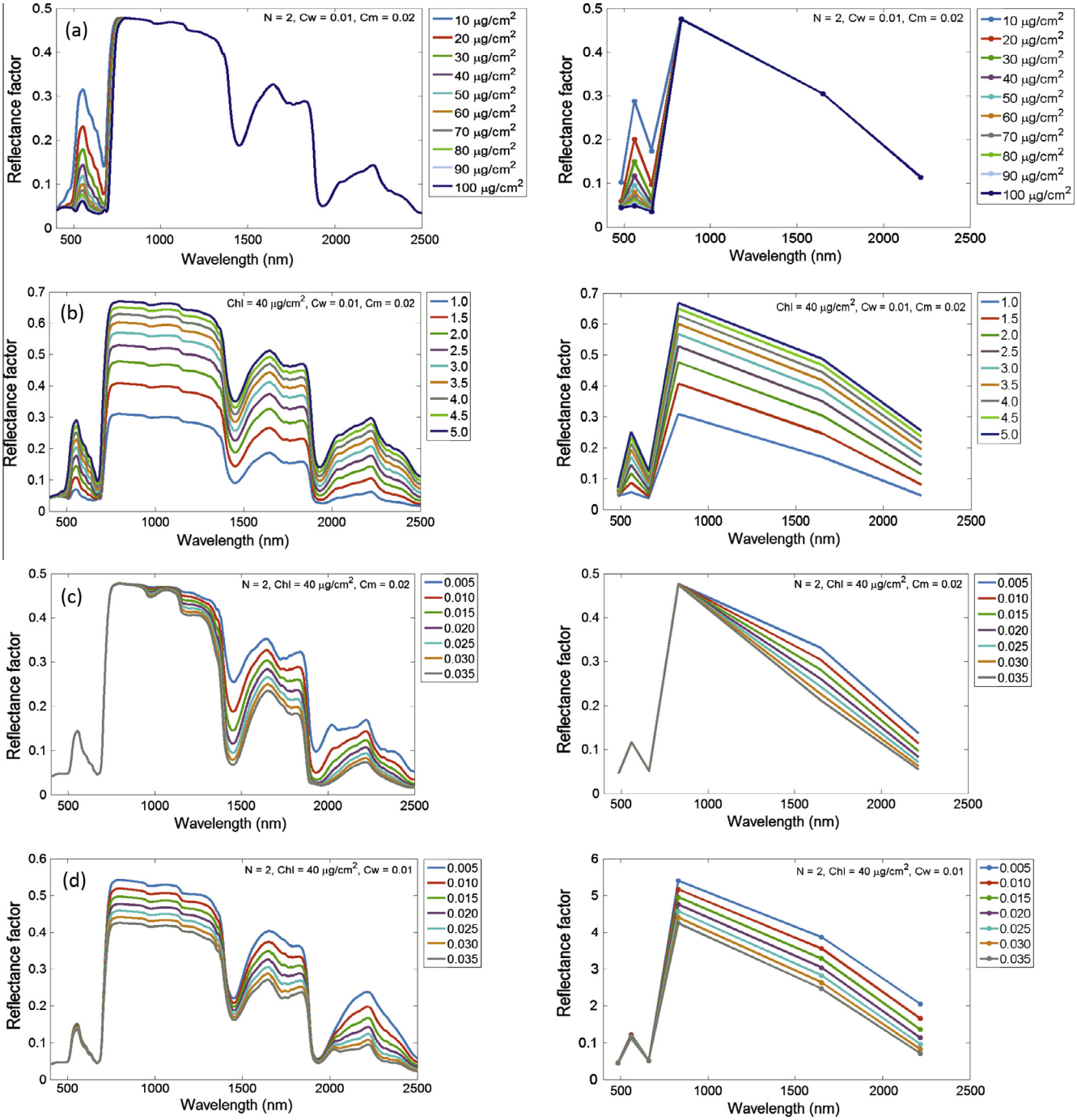

Fig. 2. PROSPECT-4 simulations for hyperspectral (left) and Landsat (right) bands where unfixed variables are (a) Chlorophyll; (b) structural parameter (N); (c) water content; (d) dry matter. The values of fixed variables are indicated within the figures.

and NIR reflectance for the same chlorophyll content (Fig. 2). The adoption of fixed structural parameters results in a considerable improvement in modelled chlorophyll, with the R^2 value increasing from $R^2 = 0.54$ to $R^2 = 0.77$ and a much greater linearity (slope = 0.42 to 0.74, intercept = 17.8 to 8.5). Importantly, the results for modelled chlorophyll using Landsat bands show extremely similar results to those from hyperspectral spectra (PROSPECT-5: $R^2 = 0.76$ and $R^2 = 0.79$, for hyperspectral and Landsat bands, respectively). This result indicates that, given the appropriate band locations, reduced and broader bands maybe used for leaf chlorophyll retrieval using radiative transfer methods.

3.3.1. Comparison between leaf-level modelled broadband chlorophyll and hyperspectral chlorophyll

To assess broadband performance relative to hyperspectral inputs, rather than a potentially coincidental relationship with measured chlorophyll, the Landsat modelled chlorophyll results are compared with hyperspectral modelled chlorophyll values. These results are also shown alongside modelled chlorophyll from bands from three other popular sensors (MERIS, MODIS and SPOT5 HRG; see Table 3 for details) to further evaluate the use of PROSPECT with differing reflectance inputs of various bandwidths, band positions, and number of bands (Fig. 4).

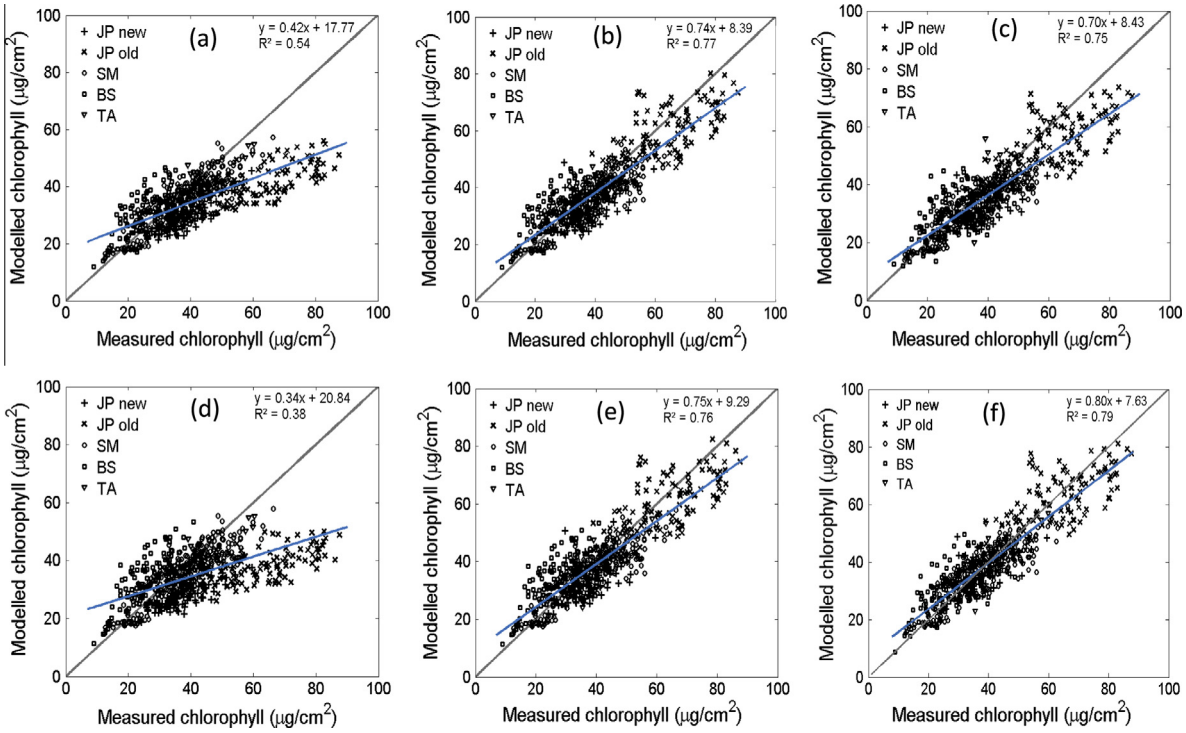

Fig. 3. Modelled leaf chlorophyll content for all species evaluated from (a) PROSPECT4 – hyperspectral structural parameter not fixed (root mean square error (RMSE) = 12.61 μg/cm^2); (b) PROSPECT4 – hyperspectral fixed structural parameter (RMSE = 8.31 μg/cm^2); (c) PROSPECT4 – Landsat bands fixed structural parameter (RMSE = 9.01 μg/cm^2); (d) PROSPECT5 hyperspectral – structural parameter not fixed (RMSE = 13.40 μg/cm^2); (e) PROSPECT5 – hyperspectral fixed structural parameter (RMSE = 7.70 μg/cm^2); (f) PROSPECT5 – Landsat bands fixed structural parameter (RMSE = 7.05 μg/cm^2). (JP – jack pine, SM – sugar maple, BS – black spruce, TA – trembling aspen).

Modelled chlorophyll content derived using Landsat, MODIS and MERIS bands all displayed a strong linear relationship with hyperspectral results, with PROSPECT5 MERIS chlorophyll showing the least scatter around the 1:1 line (R^2 = 0.99). The Landsat chlorophyll displayed slightly more scatter, but still exhibited a very strong relationship with hyperspectral chlorophyll (PROSPECT4; R^2 = 0.97) and a strong linearity (slope = 0.93, intercept = 0.78), demonstrating a lack of systematic under- or overestimation. The decreased performance using SPOT5 was likely due to the lack of a blue band and also the very broad red bandwidth (610–690 nm), which would lead to a higher red band reflectance factor and explain the under prediction in modelled chlorophyll content. Nonetheless, the still strong relationship between SPOT5 and hyperspectral chlorophyll (PROSPECT 4; R^2 = 0.96) demonstrates the limited number of reflectance bands that are needed to generate a strong performance from PROSPECT (SPOT5 = 545 nm, 645 nm and 835 nm).

3.4. Modelling leaf chlorophyll from Landsat TM satellite data

At the canopy scale, in addition to sunlit leaves, reflectance factors are also a function of non-photosynthetic elements, background material and shaded components. The results shown in Fig. 5 were produced using the 4-Scale canopy model, using the fixed parameters in Table 1, to remove the effects of confounding scene factors and retrieve leaf reflectance. The input Landsat data was taken as an average from 3 × 3 pixels centred on the ground site to reduce positional inaccuracy. Leaf chlorophyll content was subsequently modelled from modelled leaf reflectance using PROSPECT-4 and -5 retrievals.

The findings from Landsat satellite data show very strong validation results (R^2 = 0.78, RMSE = 8.73 μg/cm^2 and R^2 = 0.82, RMSE = 9.06 μg/cm^2 for P4 and P5, respectively), with a high linearity around the 1:1 line; obtaining slope values close to 1 (0.94 and 1.06) and small intercepts (1.87 and 0.75). The high comparability to leaf-level PROSPECT performance (Fig. 3) indicates that 4-scale is successfully removing the influence of canopy structural effects and background influences.

3.5. Mapped leaf chlorophyll content and leaf area index

The leaf chlorophyll content retrieval algorithm was applied over a broader, spatially continuous extent (3 km × 3 km) at 30 m resolution. Spatially continuous maps at a fine resolution may be used to monitor vegetation stress and the mechanisms controlling plant-environment interactions (Moorthy et al., 2008). The modelled leaf chlorophyll content for three locations (Haliburton, Sudbury and Chapleau) are mapped in Fig. 6 along with LAI values.

The majority of leaf chlorophyll estimates for Haliburton and Sudbury ranged from 30 to 40 μg/cm^2, which is consistent with the laboratory measured leaf-level results and previous studies (Zarco-Tejada et al., 2004a). The Chapleau location typically displayed higher chlorophyll content (≈40–50 μg/cm^2), with less local variability and clumping than the other locations, probably attributable to the presence of the pure jack pine stands. Fig. 6 shows the spatial differences in modelled leaf chlorophyll content and LAI for all three study areas, with the spatial regions of very low LAI and Chlorophyll content, attributable to lakes, water courses and roads, or areas of bare ground due to logging activity.

3.6. Spatial co-variance of LAI and leaf chlorophyll content

In an effort to investigate how LAI as an input variable and modelled leaf chlorophyll content spatially co-vary over a given area, we used bivariate Local Moran's *I* statistic to identify spatial clusters in the data (Anselin, 1995; Sunderlin et al., 2008). A measure of the statistical significance of the relationship between the two

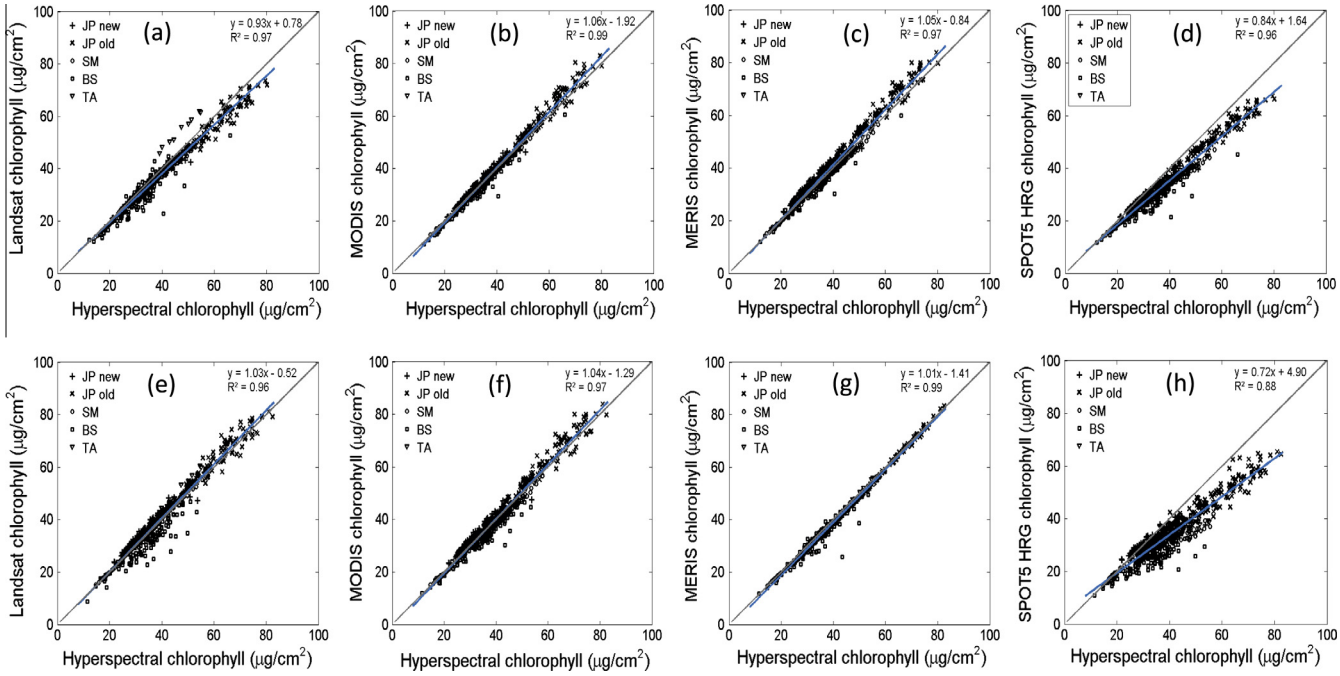

Fig. 4. Comparison of PROSPECT 4 hyperspectral derived chlorophyll with modelled chlorophyll from (a) Landsat 5 TM (root mean square error (RMSE) = 3.01 μg/cm^2); (b) MODIS (RMSE = 1.80 μg/cm^2); (c) MERIS (RMSE = 2.50 μg/cm^2); (d) SPOT5 HRG (RMSE = 5.38 μg/cm^2) and PROSPECT 5 hyperspectral modelled chlorophyll against modelled chlorophyll from (e) Landsat 5 TM (RMSE = 2.77 μg/cm^2); (f) MODIS (RMSE = 2.39 μg/cm^2); (g) MERIS (RMSE = 1.63 μg/cm^2); (h) SPOT5 HRG (RMSE = 7.75 μg/cm^2). (JP – jack pine, SM – sugar maple, BS – black spruce, TA – trembling aspen).

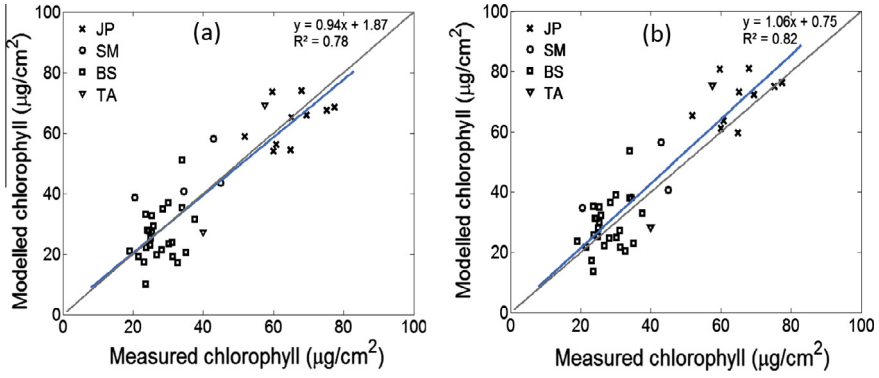

Fig. 5. Leaf chlorophyll content for all species evaluated from Landsat imagery modelled using the 4-Scale canopy model linked with (a) PROSPECT4 ($p < 0.001$; root mean square error (RMSE) = 8.73 μg/cm^2) and (b) PROSPECT5 ($p < 0.001$; RMSE = 9.06 μg/cm^2). (JP – jack pine, SM – sugar maple, BS – black spruce, TA – trembling aspen).

spatial LAI and leaf chlorophyll datasets was then derived from spatially randomised reference distributions of local Moran's *I* values to observed values, and is shown in Fig. 7 at a range of confidence intervals (Anselin et al., 2006).

Perhaps unsurprisingly, Fig. 7 reveals the presence of significant spatial correlations between areas of low LAI values or bare ground and low leaf chlorophyll content in the pixel, due to the lack of leaves present. Another notable spatial basis of significant relationships are regions of high LAI and high chlorophyll content (Fig. 6), for example the north-east corner of the Chapleau site (Fig. 7c). This could be due an isolated patch of different tree species, or a result of stand age controls on both LAI and chlorophyll (Croft et al., 2014a). Importantly, Fig. 7 shows large regions of non-significant relationships (where $p > 0.05$) between the two variables across all three sites, and variations in the spatial patterns of correlations. This result indicates the that the algorithm is robust and leaf chlorophyll predictions are not due to a over-dependence on LAI values.

4. Discussion

As demonstrated in Fig. 3, the structural variables for the jack pine leaves (*N* parameter to 3.5 for new leaves and 5 for old leaves) had to be fixed to prevent an underestimation of chlorophyll content. The effects of the *N* parameter on leaf reflectance can be seen in Fig. 2, which illustrates that for the same chlorophyll content, reflectance factors will be higher in both red and NIR wavelengths. Previous studies have highlighted the unsuitability of PROSPECT for needle leaved species because the assumption of infinite planes is violated for needle leaves, which have adaxial and abaxial surfaces that are not flat planes or are not horizontally infinite (Zhang et al., 2008b). PROSPECT considers light transfer between internal plates isotropically, however the needle thickness is similar to needle width leading to potentially large losses in light through leaf edges. Zhang et al. (2008b) found light scattered isotropically in visible wavelengths, but predominately forward-scattered in NIR. Despite black spruce and jack pine having similar

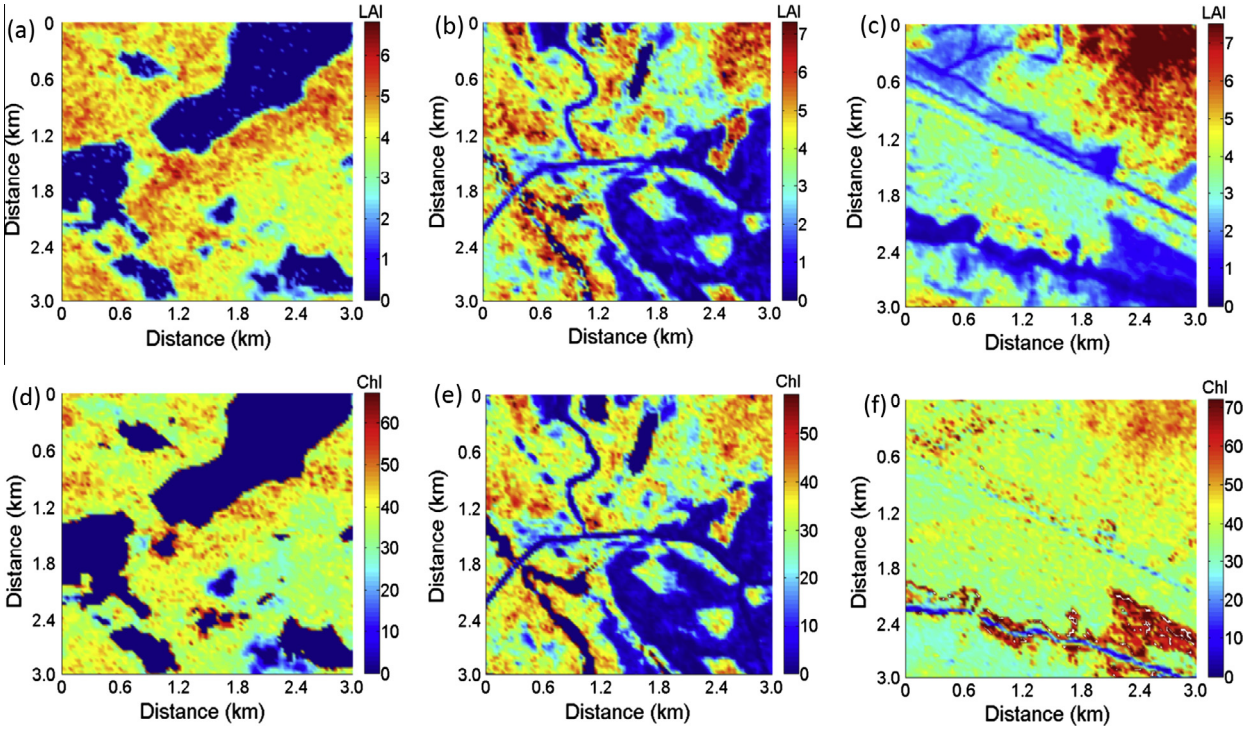

Fig. 6. Mapped leaf area index for (a) Haliburton, (b) Sudbury, (c) Chapleau and leaf chlorophyll content for (d) Haliburton, (e) Sudbury, (f) Chapleau sites.

leaf thicknesses, jack pine needle reflectance factors in both visible and NIR wavelengths are considerably higher than those of black spruce needles (Fig. 1). This higher jack pine reflectance is contrary to what we might expect given its chlorophyll content is approximately 50% higher (mean chlorophyll content; BS = 40.66 μg/cm^2 and JP old = 63.36 μg/cm^2). Reducing leaf structural effects to leaf thickness may be an oversimplification, given that leaf structure also includes the fraction of intercellular airspace, the ratio of cell walls to intercellular space, and epidermal and mesophyll cell dimensions (Ollinger, 2011; Serrano, 2008). In effect, the *N* parameter encompasses all of these factors into one value, which represents the number of mesophyll air/cell interfaces, although this makes it difficult to actually measure (Ollinger, 2011). Another explanation for higher than expected jack pine reflectance may be the presence of a thicker epicuticular wax, or a different wax morphology or chemical composition that is increasing leaf surface reflectance but is unrelated to internal leaf biochemical or physical variables. Further work into the relationship between internal leaf structure, leaf pigments, surface composition and reflectance factors for jack pine and other needle leaves is required to address this issue.

Despite the small number of Landsat bands used in the PROSPECT inversion simulations and their large bandwidths, the predicted chlorophyll results showed a surprisingly high accuracy when compared to corresponding hyperspectral inputs (R^2 = 0.97, RSME = 3.01 μg/cm^2). This may be due to the high redundancy of wavelength channels in vegetation studies (Jacquemoud et al., 1995; Simic and Chen, 2008). Thenkabail et al. (2004) found that data volume can be reduced by 97% when hyperspectral wavebands are reduced to the first five principal components, and still explain close to 95% variability in data. They identified seven optimal bands (495 nm, 555 nm, 655 nm, 675 nm, 705 nm, 915 nm, and 985 nm for vegetation studies. In a mathematical context, a greater difficulty with the use of some multispectral sensors in radiative transfer modelling may be the limited number of bands present, particularly when the input bands is similar or equal to the number of predicted variables (Jacquemoud et al., 1995). In this study, the use of bounded restrictions (Table 2) improved the accuracy of the modelled chlorophyll results using Landsat bands, reducing the number of spurious predictions. Nonetheless, our findings, with over 600 leaf samples tested, comprehensively demonstrate the strong performance of PROSPECT, and confirm

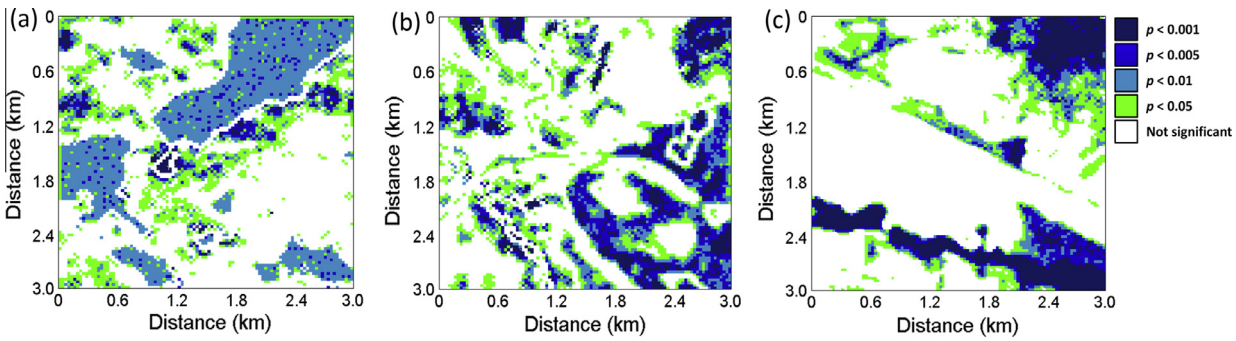

Fig. 7. The statistical significance in patterns of spatial correlation between LAI and leaf chlorophyll content, derived from local Moran's *I* statistic.

the findings of Jacquemoud et al. (1995) who showed that chlorophyll retrievals were very similar from 188 AVIRIS narrow bands and 6 Landsat bands (root mean square error (RMSE) = 18 μg/cm^2 and 15 μg/cm^2, respectively) over sugar beet canopies. It is expected that more complex radiative transfer models, which require a greater number of inversion parameters, may not be suitable for the limited number of input bands available from multispectral sensors.

The slight differences in the chlorophyll prediction results from PROSPECT-4 and -5 using hyperspectral bands confirmed the findings of Feret et al. (2008), with leaf-level PROSPECT-5 predictions slightly exceeding PROSPECT-4 for hyperspectral and Landsat bands (Landsat: R^2 = 0.75 and 0.79 for PROSPECT-4 and -5, respectively). Feret et al. (2008) also found a slight improvement for PROSPECT-5 (RMSE = 9 μg/cm^2) compared to PROSPECT-4 (RMSE = 10 μg/cm^2) and attributed this slight improvement to better modelling of leaves with low chlorophyll content, and offsetting of the presence of carotenoids by PROSPECT-4 by an overestimation of chlorophyll. Our study provides some support for this with a slightly reduced PROSPECT-5 intercept value (7.4 and 8.5 for PROSPECT-5 and -4, respectively) although the differences are relatively small. Surprisingly, the differences between chlorophyll modelled from Landsat and hyperspectral bands was small given the increased bandwidth, although this could be attributable to the presence of the blue Landsat band (450–520 nm), which captures much of the carotenoid signal. The RMSE (7.05 and 7.70 μg/cm^2 for Landsat and hyperspectral, respectively) was very close to those found by Feret et al., 2008 (RMSE = 9 μg/cm^2), despite the inclusion of both needle and broadleaf species.

The mapped leaf chlorophyll content and LAI for sites at the three study areas shown in Fig. 6 reveals the spatial differences in the two variables. The large areas of extreme low LAI values correspond to lakes and areas of bare ground and the lack of trees explains the lack of leaf chlorophyll content. However, there is also a large degree of spatial independence between LAI and modelled leaf chlorophyll in the forested regions (Fig. 7), which is an important finding because LAI is derived from the same sensor as used to model chlorophyll and is also a fundamental variable parameter used to drive the 4-Scale inversion. The spatial independence of the two variables is attributable to the inclusion of the Landsat SWIR band in the empirical LAI modelling, which is not used in chlorophyll modelling and provides a separate and independent source of data. There does appear to be some localised areas of very high chlorophyll content, particularly surrounding water bodies and roads. This could be a result of variations in the landscape vegetation composition that does not match the fixed parameters in Table 1, for example the presence of different tree species and background composition or variations in canopy structural variables that deviate from the fixed structural parameters, as demonstrated by Figs. 6 and 7. This highlights a challenge for modelling leaf chlorophyll using physically-based algorithms, because the representative fixed parameters do not always reflect the variables within the landscape. Background vegetation for example, has its own phenology and varies spatially with canopy structure. Whilst further progress is needed to develop the technologies for supplying spatially-distributed information on canopy structure and background composition, a physically-based approach represents the opportunity to theoretically account for these confounding variables, in comparison to empirical approaches which are largely site, time and species specific (Croft et al., 2014c). Despite these challenges, the relationship between measured and modelled chlorophyll from Landsat satellite data for the validation sites is very good (R^2 = 0.78; RMSE = 8.73 μg/cm^2). In comparison, vegetation indices have shown similar strong performances over homogenous, closed forests with one vegetation type (e.g. Datt, 1998, R^2 = 0.83). Zarco-Tejada et al. (2004b) demonstrated that for open canopies the relationship between vegetation index and leaf chlorophyll is lower (R^2 = 0.35), unless the spatial resolution is fine enough to allow the separation of vegetation crowns from other scene components (increasing the result to R^2 = 0.69). The fine spatial resolution of the Landsat map (30 m) reveals the degree of localized spatial variation in leaf chlorophyll in forested areas across the landscape and permits representation of local controls on the spatial variability in pigment content such as soil nutrient content, soil moisture content, topography, leaf/stand age and vegetation stress.

5. Conclusion

This research demonstrates the potential to use data from Landsat 5 TM and other multispectral sensors to predict leaf chlorophyll content using a physical modelling approach. The accuracy of PROSPECT chlorophyll predictions using simulated Landsat bands was assessed against hyperspectral results, and a very strong relationship (R^2 = 0.97) and negligible differences (RMSE = 3.01 μg/cm^2) were found. This relationship was confirmed using simulated bands from other sensors, i.e., MERIS (RMSE = 1.80 μg/cm^2) and MODIS (RMSE = 2.50 μg/cm^2), with only SPOT5 displaying notably poorer performance (RMSE = 5.38 μg/cm^2), i.e., underestimations at higher chlorophyll contents. The same strong results were found when tested on Landsat satellite data (R^2 = 0.78; RMSE = 8.73 μg/cm^2), using a 4-Scale canopy reflectance model to model leaf reflectance and subsequent PROSPECT inversion to derive leaf chlorophyll. Very similar results were found for PROSPECT-4 and PROSPECT-5 for both hyperspectral and multispectral leaf-level inputs and also for canopy-coupled inversions (e.g., canopy R^2 = 0.78 and 0.82 for P4 and P5, respectively), although the higher number of inversion parameters for PROSPECT-5 relative to the limited input bands could result in errors in the inversion process. Bounded variable ranges were required in the inversion. The application of this algorithm at the fine spatial resolution (30 m) that Landsat offers provides considerable possibilities for promoting a better understanding of leaf pigment dynamics at fine spatial resolutions and over decadal timescales.

References

Anselin, L., 1995. Local indicators of spatial association—LISA. Geogr. Anal. 27, 93–115.
Anselin, L., Syabri, I., Kho, Y., 2006. GeoDa: an introduction to spatial data analysis. Geogr. Anal. 38, 5–22.
Chander, G., Markham, B., 2003. Revised Landsat-5 TM radiometric calibration procedures and postcalibration dynamic ranges. Geosci. Remote Sens., IEEE Trans. 41, 2674–2677.
Chavez Jr, P.S., 1988. An improved dark-object subtraction technique for atmospheric scattering correction of multispectral data. Remote Sens. Environ. 24, 459–479.
Chavez Jr, P.S., 1996. Image-based atmospheric corrections-revisited and improved. Photogramm Eng Remote Sens. 62, 1025–1036.
Chen, J.M., Cihlar, J., 1995. Quantifying the effect of canopy architecture on optical measurements of leaf area index using two gap size analysis methods. Geosci. Remote Sens., IEEE Trans. 33, 777–787.
Chen, J.M., Leblanc, S.G., 1997. A four-scale bidirectional reflectance model based on canopy architecture. Geosci. Remote Sens., IEEE Trans. 35, 1316–1337.
Chen, J.M., Leblanc, S.G., 2001. Multiple-scattering scheme useful for geometric optical modeling. Geosci. Remote Sens., IEEE Trans. 39, 1061–1071.
Chen, J.M., Plummer, P.S., Rich, M., Gower, S.T., Norman, J.M., 1997. Leaf area index measurements. J. Geophys. Res. 102, 29–429.
Chen, F., Niu, Z., Sun, G., Wang, C., Teng, J., 2008. Using low-spectral-resolution images to acquire simulated hyperspectral images. Int. J. Remote Sens. 29, 2963–2980.
Croft, H., Anderson, K., Brazier, R.E., Kuhn, N.J., 2013a. Modeling fine-scale soil surface structure using geostatistics. Water Resour. Res. 49, 1858–1870.
Croft, H., Chen, J.M., Zhang, Y., Simic, A., 2013b. Modelling leaf chlorophyll content in broadleaf and needle leaf canopies from ground, CASI, Landsat TM 5 and MERIS reflectance data. Remote Sens. Environ. 133, 128–140.
Croft, H., Chen, J., Noland, T., 2014a. Stand age effects on Boreal forest physiology using a long time-series of satellite data. For. Ecol. Manage. 328, 202–208.

Croft, H., Chen, J.M., Zhang, Y., 2014b. Temporal disparity in leaf chlorophyll content and leaf area index across a growing season in a temperate deciduous forest. Int. J. Appl. Earth Obs. Geoinf. 33, 312–320.
Croft, H., Chen, J.M., Zhang, Y., 2014c. The applicability of empirical vegetation indices for determining leaf chlorophyll content over different leaf and canopy structures. Ecol. Complex. 17, 119–130.
Datt, B., 1998. Remote sensing of chlorophyll a, chlorophyll b, chlorophyll a+b, and total carotenoid content in eucalyptus leaves. Remote Sens. Environ. 66, 111–121.
Demarez, V., Gastellu-Etchegorry, J.P., 2000. A modeling approach for studying forest chlorophyll content. Remote Sens. Environ. 71, 226–238.
Feret, J.B., François, C., Asner, G.P., Gitelson, A.A., Martin, R.E., Bidel, L.P.R., Ustin, S.L., le Maire, G., Jacquemoud, S., 2008. PROSPECT-4 and 5: advances in the leaf optical properties model separating photosynthetic pigments. Remote Sens. Environ. 112, 3030–3043.
Gitelson, A.A., Viña, A., Verma, S.B., Rundquist, D.C., Arkebauer, T.J., Keydan, G., Leavitt, B., Ciganda, V., Burba, G.G., Suyker, A.E., 2006. Relationship between gross primary production and chlorophyll content in crops: Implications for the synoptic monitoring of vegetation productivity. J Geophys Research D: Atmos. 111.
Gradowski, T., Thomas, S.C., 2006. Phosphorus limitation of sugar maple growth in central Ontario. For. Ecol. Manage. 226, 104–109.
Houborg, R., Boegh, E., 2008. Mapping leaf chlorophyll and leaf area index using inverse and forward canopy reflectance modeling and SPOT reflectance data. Remote Sens. Environ. 112, 186–202.
Houborg, R., Anderson, M., Daughtry, C., 2009. Utility of an image-based canopy reflectance modeling tool for remote estimation of LAI and leaf chlorophyll content at the field scale. Remote Sens. Environ. 113, 259–274.
Inoue, Y., Peñuelas, J., Miyata, A., Mano, M., 2008. Normalized difference spectral indices for estimating photosynthetic efficiency and capacity at a canopy scale derived from hyperspectral and CO2 flux measurements in rice. Remote Sens. Environ. 112, 156–172.
Jacquemoud, S., Baret, F., 1990. PROSPECT: A model of leaf optical properties spectra. Remote Sens. Environ. 34, 75–91.
Jacquemoud, S., Baret, F., Andrieu, B., Danson, F.M., Jaggard, K., 1995. Extraction of vegetation biophysical parameters by inversion of the PROSPECT+SAIL models on sugar beet canopy reflectance data. Application to TM and AVIRIS sensors. Remote Sens. Environ. 52, 163–172.
Jacquemoud, S., Verhoef, W., Baret, F., Bacour, C., Zarco-Tejada, P.J., Asner, G.P., François, C., Ustin, S.L., 2009. PROSPECT + SAIL models, A review of use for vegetation characterization. Remote Sens. Environ. 113 (1), S56–S166.
Kimes, D.S., Knyazikhin, Y., Privette, J.L., Abuelgasim, A.A., Gao, F., 2000. Inversion methods for physically-based models. Remote Sens. Reviews 18, 381–439.
Kovalskyy, V., Roy, D.P., 2013. The global availability of Landsat 5 TM and Landsat 7 ETM + land surface observations and implications for global 30 m Landsat data product generation. Remote Sens. Environ. 130, 280–293.
Kuusk, A., 1995. A Markov chain model of canopy reflectance. Agric. For. Meteorol. 76, 221–236.
Leithead, M., Silva, L.C.R., Anand, M., 2012. Recruitment patterns and northward tree migration through gap dynamics in an old-growth white pine forest in northern Ontario. Plant Ecol. 213, 1699–1714.
Malenovský, Z., Homolová, L., Zurita-Milla, R., Lukeš, P., Kaplan, V., Hanuš, J., 2013. Gastellu-Etchegorry, JP. and Michael E Schaepman, M.E., Retrieval of spruce leaf chlorophyll content from airborne image data using continuum removal and radiative transfer. Remote Sens. Environ. 131, 85–102.
Moorthy, I., Miller, J.R., Noland, T.L., 2008. Estimating chlorophyll concentration in conifer needles with hyperspectral data, an assessment at the needle and canopy level. Remote Sens. Environ. 112, 2824–2838.
Ollinger, S.V., 2011. Sources of variability in canopy reflectance and the convergent properties of plants. New Phytol. 189, 375–394.
Richardson, A.D., Duigan, S.P., Berlyn, G.P., 2002. An evaluation of noninvasive methods to estimate foliar chlorophyll content. New Phytol. 153, 185–194.
Rowe, J.S., 1972. Forest regions of Canada. Information Canada.
Sampson, P.H., Zarco-Tejada, P.J., Mohammed, G.H., Miller, J.R., Noland, T.L., 2003. Hyperspectral remote sensing of forest condition: estimating chlorophyll content in tolerant hardwoods. For. Sci. 49, 381–391.
Serrano, L., 2008. Effects of leaf structure on reflectance estimates of chlorophyll content. Int. J. Remote Sens. 29, 5265–5274.
Simic, A., Chen, J.M., 2008. Refining a hyperspectral and multiangle measurement concept for vegetation structure assessment. Can. J. Remote Sens. 34, 174–191.
Simic, A., Chen, J.M., Noland, T.L., 2011. Retrieval of forest chlorophyll content using canopy structure parameters derived from multi-angle data: the measurement concept of combining nadir hyperspectral and off-nadir multispectral data. Int. J. Remote Sens. 32, 5621–5644.
Steven, M.D., Malthus, T.J., Baret, F., Xu, H., Chopping, M.J., 2003. Intercalibration of vegetation indices from different sensor systems. Remote Sens. Environ. 88, 412–422.
Sunderlin, W.D., Dewi, S., Puntodewo, A., Müller, D., Angelsen, A., Epprecht, M., 2008. Why forests are important for global poverty alleviation: a spatial explanation. Ecol. Soc. 13, 24–45.
Thenkabail, P.S., Enclona, E.A., Ashton, M.S., Van Der Meer, B., 2004. Accuracy assessments of hyperspectral waveband performance for vegetation analysis applications. Remote Sens. Environ. 91, 354–376.
Tobler, W., 1965. Computation of the correspondence of geographical patterns. Papers Regional Sci. Assoc. 15, 131–139.
Verrelst, J., Muñoz, J., Alonso, L., Delegido, J., Rivera, J.P., Camps-Valls, G., Moreno, J., 2012. Machine learning regression algorithms for biophysical parameter retrieval: opportunities for Sentinel-2 and -3. Remote Sens. Environ. 118, 127–139.
Vogelmann, J.E., Rock, B.N., Moss, D.M., 1993. Red edge spectral measurements from sugar maple leaves. Int. J. Remote Sens. 14, 1563–1575.
Wellburn, A.R., 1994. The spectral determination of chlorophylls a and b, as well as total carotenoids, using various solvents with spectrophotometers of different resolution. J. Plant Physiol. 144, 307–313.
Zarco-Tejada, P.J., Miller, J.R., Mohammed, G.H., Noland, T.L., Sampson, P.H., 2002. Vegetation stress detection through chlorophyll a + b estimation and fluorescence effects on hyperspectral imagery. J. Environ. Qual. 31, 1433–1441.
Zarco-Tejada, P.J., Miller, J.R., Harron, J., Hu, B., Noland, T.L., Goel, N., Mohammed, G.H., Sampson, P., 2004a. Needle chlorophyll content estimation through model inversion using hyperspectral data from boreal conifer forest canopies. Remote Sens. Environ. 89, 189–199.
Zarco-Tejada, P.J., Miller, J.R., Morales, A., Berjón, A., Agüera, J., 2004b. Hyperspectral indices and model simulation for chlorophyll estimation in open-canopy tree crops. Remote Sens. Environ. 90, 463–476.
Zhang, Y., Chen, J.M., Thomas, S.C., 2007. Retrieving seasonal variation in chlorophyll content of overstory and understory sugar maple leaves from leaf-level hyperspectral data. Can. J. Remote Sens. 33, 406–415.
Zhang, Y., Chen, J.M., Miller, J.R., Noland, T.L., 2008a. Leaf chlorophyll content retrieval from airborne hyperspectral remote sensing imagery. Remote Sens. Environ. 112, 3234–3247.
Zhang, Y., Chen, J.M., Miller, J.R., Noland, T.L., 2008b. Retrieving chlorophyll content in conifer needles from hyperspectral measurements. Can. J. Remote Sens. 34, 296–310.
Zhu, Z., Foster, N.W., Arp, P.A., Meng, F., Bourque, C.P.A., 2004. A test and application of the model ForNBM in a northeastern Ontario jack pine (*Pinus banksiana* lamb.) stand. For. Ecol. Manage. 193, 385–397.